OPTICAL STUDY ON NEEDLE LIFT AND ITS EFFECTS ON REACTING DIESEL SPRAYS OF A SINGLE-HOLE SOLENOID INJECTOR

Tiemin Xuan[1,3], Zhongcheng Sun[1], Peng Lu[1], Wenjun Zhong[1], Zhanbo Si[1], Zhixia He[2]*, Qian Wang[1]*, Zhou Chen[1], Wei Guan[1]

[1] School of Energy and Power Engineering, Jiangsu University, Zhenjiang 212013, China

[2] Institute for Energy Research, Jiangsu University, Zhenjiang 212013, China

[3] CSSC Marine Power Co, LTD, Zhenjiang 212002, China

* Corresponding author: Zhixia He, Email: zxhe@ujs.edu.cn , Wang, Email: qwang@ujs.edu.cn

Precise control of needle lift provides one possibility to control the Diesel spray and combustion process actively. However, most studies of needle lift focus on internal flow or near nozzle spray. Little work has been performed on its effects on reacting spray. In this work, one way to change the needle lift profile of a solenoid injector has been developed and the relationship between needle lift and reacting spray has been investigated. The needle movement was detected with an optical nozzle. In addition, the visualization of reacting sprays of the same injector equipped with a single-hole nozzle was conducted in a combustion chamber. Some simulations were also performed to assist the analysis. The results show that the needle lift profile can be regulated by changing the thickness of an adjusting pad. It seems the different needle lift profiles do not bring in significant influences on reacting spray characteristics. The CFD results indicate that it is mainly caused by the similar internal flow characteristics which do not show strong variation when needle lift is higher than 0.1 mm. However, the discharge coefficient and velocity coefficient decrease sharply when needle lift is smaller than 0.05 mm because of the "throttle" effect.

Keywords: needle lift; reacting Diesel spray; single-hole; optical techniques

1 Introduction

Fuel-air mixing plays a significant role in Diesel engine combustion process. The complexity of this phenomenon has been a significant challenge to the researchers boosting investigations in this area. Precise control of injection event contributes greatly to the optimization of fuel-air mixing process, as well as engine performances and pollutant emissions [1,2]. In the last few decades, substantial experimental and computational works have been made in order to achieve the ideal sprays. Nowadays, the injection timing and fuel quantity distribution can be controlled in a flexible way by means of the high pressure electronically controlled common rail systems. Thanks to that, various injection rate shapes [3-4] and multiple injection strategies [5-6] have been studied to get a better fuel-air mixing and more homogeneous combustion. The effect of nozzle geometry (such as conicity, inlet rounding, nozzle hole numbers) on mixture formation and combustion of the diesel spray has also been an

interest field to the research community and the automotive manufacturer [7]. In addition, the cavitation inside the nozzle could bring a significant influence on Diesel spray development, as well as combustion process, which has also been investigated a lot in recent years in order to control the spray actively [8-11].

Besides above methodologies, a better understanding of the effects of needle lift on spray development could provide another possibility to control fuel-air mixing and combustion process more effectively. Some studies on the needle lift movement have been carried out experimentally. Most of them were performed by means of X-ray phase-enhanced imaging [12-13]. However, most of them focus on internal flow or near-nozzle dense sprays and the cost for these experiments are quite expensive. Some numerical works have also been carried out on the influence of needle lift on the internal flow and cavitation phenomenon [14,15]. They found that the main flow features as well as cavitation appearance present difference at different partial needle lifts. In addition, a few works also studied the effects of needle lift on non-reacting spray characteristics. R. Payri et al. investigated the needle lift profile influence on liquid length [16] and vapor phase penetration [17] of non-reacting sprays through a piezoelectric injector equipped with a multi-hole nozzle. In their studies, the needle position is believed to be regulated by changing the charge applied to the piezo-stack. Nevertheless, the real needle movement was not detected. As mentioned above, the target of studying needle lift is to control fuel-air mixing and consequent combustion process more effectively. However, it can be found from previous literatures that the studies on needle lift are limited to needle motion and internal flow of piezoelectric injectors. No information is found for solenoid injector because its needle lift is not able to be controlled as flexible as piezoelectric injector. Furthermore, to the best of our knowledge, no study has been done on the effects of needle lift on combustion process. Thus, it will be very important to link the needle lift measurement and reacting spray characteristics.

2 Materials and methods

The experimental measurements of this study can be divided into two parts: needle lift visualization and spray visualization. The injector performed in these two kinds of tests is the same one, a solenoid BOSCH injector. The only difference is an optical nozzle tip is used to visualize needle movement, while a normal metal nozzle is used for spray visualization. It needs to be pointed out that two holes have been produced for optical nozzle because the material is too easy to be broken with a single hole. In order to change the maximum needle lift (NL_{max}), an adjusting pad was mounted between needle and rod as shown in Fig. 1. Thus, the NL_{max} can be regulated by changing the thickness of the pad.

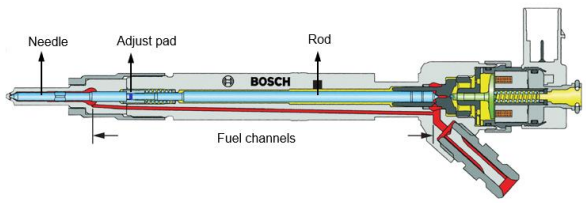

Fig. 1 Schematic of adjusting pad position

2.1 Needle lift visualization

In this part, in order to capture the transient needle movement, the metal nozzle tip of injector was cut and replaced by a real-size optical acrylic nozzle tip, considering its good light transmittance (> 92%), good compression resistance and similar refractive index (1.49) to diesel fuel (around 1.475). The schematic of this visualization system is presented in Fig. 2. A LED was applied as the light source and a high-speed CMOS camera equipped with a long-distance microscope (QM-1, QUESTAR) was placed at the opposite side running at 100,000 frames per second (fps) to record the needle movement. A common rail injection system was applied to supply high pressure fuel, while the ambient pressure of all injections is atmospheric pressure.

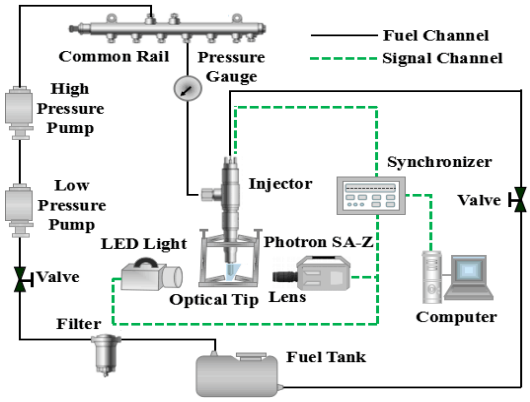

Fig. 2 Schematic of visualization system for needle lift [8].

2.2 Spray visualization

The spray visualization experiments were carried out in a pre-heated constant volume combustion chamber which is able to simulate the in-cylinder conditions of diesel engines at TDC position. This test chamber can maintain the stationary conditions with the maximum ambient temperature of 900 K and a maximum pressure of 6 MPa. It is equipped with four optical windows (92 mm in diameter) placed orthogonally with a thickness of 76 mm. The detailed information of this chamber can be found in reference [18,19]. The same fuel injector as mentioned above was also used here equipped with a single-hole nozzle in 120 μm diameter. The injector was placed at the center of the main port of Constant Volume Combustion Chamber (CVCC). A high-speed Schlieren imaging and OH* chemiluminescence were performed in this test rig to record spray geometry and flame lift-off length (LOL), respectively. The schematic of this CVCC and optical arrangement are shown in Fig. 3.

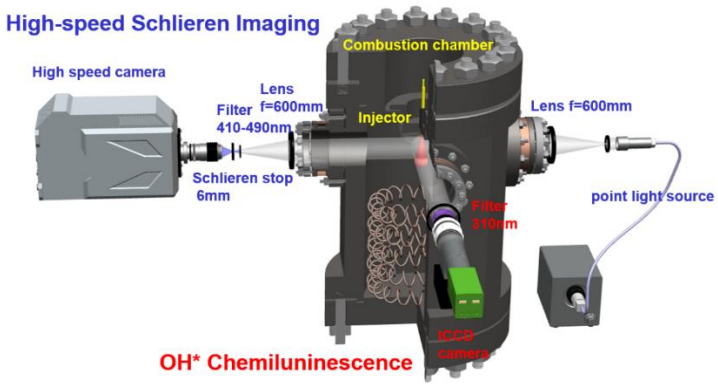

Fig. 3 CVCC and optical arrangement

2.2.1 High-speed Schlieren Imaging

The actual Schlieren optical setup is shown in Fig. 3. A point light obtained from a lamp was collimated by a spherical lens (f=600mm) which directs it through the combustion chamber. Another same spherical lens was placed on the other side of the chamber to focus the light onto a Fourier plane. A diaphragm (6 mm) was used as Schlieren stop so that the light is later collected by a high speed-CMOS camera (Phatron SA-Z) running at 60,000 frames per second (fps). As for the reacting spray measurement, in order to eliminate the soot radiation effect, a bandpass filter (410-490 nm) was placed in front of the Schlieren stop (as shown in Fig. 3) and the shutter time is reduced to 1.25 μs compared with 3.47 μs for non-reacting spray, while the other settings were kept the same with non-reacting one.

In addition, ignition delay (ID) was also obtained from Schlieren images based on the analysis on the total intensity increment within the spray between each two following images [20,21], where the corresponding time of the peak of the total intensity increment was defined as ignition delay.

2.2.2 OH chemiluminescence*

Lift-off length was measured by recording the signal from OH* chemiluminescence, being a marker of the diffusion flame limits. A schematic of the actual optical setup is also shown in Fig. 3. The time-averaged light emission near 310 nm dominated by OH chemiluminescence was acquired with an intensified charge-coupled device camera (Nikon Hisence MK) fitted with a 310 nm band-pass filter (10 nm FHWM) and a UV lens (Nikkor 105-mm f/2.8). Time-averaging images were accomplished by using a constant intensifier gating time window synchronized with the injection between 2.5 and 4.0 ms after the start of the injections (ASOI): in this way the shot-to-shot deviation was reduced. Once images are captured, the post-processing follows the approach presented in [22,23].

2.3 Test plan

The operating points for need lift visualization are summarized in Tab.1. Besides the original needle lift evolution (NLOR, without mounting any pads), four pads with different thickness have been mounted in the injector to obtain four different maximum needle lift (NL0.1, NL0.2, NL0.3, NL0.4).

The NL_{max} presented in Tab.1 is just an approximate value which can be a little different with different injection pressure, while the NL_{max} of NLOR case cannot be detected because it exceeds the limitation of optical access. Three injection pressures have been performed for each operating point, with an energizing time (ET) 2 ms. It needs to be noted that the injection pressure for needle lift visualization is relatively lower than those for spray visualization tests because the optical nozzle tip is too fragile to support high hydraulic pressure. An averaged needle moving curve out of five repetitions has been obtained for each operating point.

Tab. 1 Test plan of needle lift visualization

Operating Point	Thickness of pad [mm]	NL_{max} [mm]	ET [ms]	P_{inj} [MPa]
NL0.1	0.8	~0.1	2	50/60/70
NL0.2	0.7	~0.2	2	50/60/70
NL0.3	0.6	~0.3	2	50/60/70
NL0.4	0.5	~0.4	2	50/60/70
NLOR	-	>0.6	2	50/60/70

The investigated operating conditions for spray visualization are summarized in Tab.2. The parametric variation in injection pressure (p_{inj}) and ambient temperature (T_a) were performed by injecting the fuel into pure nitrogen or into a 18% oxygen exhaust gas recirculation environment mixed with nitrogen, while the ambient density (ρ_a) was kept constant as 21.4 kg/m3. As mentioned above, a common rail solenoid injector equipped with a single hole nozzle (d0 = 120 μm) was applied in this study and fuel used for both spray and need lift visualization is commercial diesel (China's Diesel No.0). Two different NLmax cases (NLOR, NL0.1) have been carried out for all operating points presented in Tab.2. In order to have the same injection duration (around 4 ms), the energizing time was set as 2.1 and 3.5 ms for NLOR and NL0.1, respectively. In order to improve the statistical reliability of the results presented, 10 injection cycles were recorded for each operating condition.

Tab. 2 Test plan of spray visualization

T_a [K]	p_{inj} [MPa]	ρ_a [kg/m3]	p_a [MPa]	O_2 [%(vol)]
890	110	21.4	5.49	18
850	70, 110,150	21.4	5.41, 5.25	0,18
810	110	21.4	5	18

3 Results

3.1 Needle lift movement

The effects of adjusting pad on needle lift are presented in Fig. 4, where the movement curves have been fitted by linear functions. It can be observed that the needle of NLOR case has started closing before it reaches the optical limitation with present injection pressure and energizing time. The

experimental images corresponding to Fig. 4 (a) at the time of needle closing are shown in Fig. 4 (b), where the black areas with the nozzles are caused by string cavitation [8,24] or geometry cavitation[9,10,25]. In other words, in terms of inclined-hole nozzles, different NL_{max} could lead to different internal flow characteristics, which could bring an important influence on subsequent spray evolution. However, owing to the mechanical limitation of CVCC, a single vertical-hole nozzle was conducted preliminarily for spray analysis in later section. It can be found from Fig. 4 that the maximum needle lift can be controlled well by changing the thickness of the adjusting pad.

As shown in Fig. 4 (a), with higher NL_{max} it seems the needle opening speed is a little faster. However, the time needed for reaching the NL_{max} is still a little later because of longer displacement. On the other hand, the difference of NL_{max} does not bring a significant influence on the starting time of needle closing with the same injection pressure and energizing time, namely, the mechanical delay to the electronic signal is kept same. One interesting phenomenon can be observed from Fig. 4(a) that movement lines for needle closing are almost parallel. Thus, the time needed for needle closing as a function of NL_{max} under all operating points are presented in Fig. 5. It shows a pretty linear relationship between the closing time and NL_{max}. As a consequence, it can be summarized that the higher NL_{max} leads to a faster needle opening speed, but it does not have significant effects on needle closing speed. It can also be discovered that, in order to keep the same injection duration, a longer energizing time is needed for smaller NL_{max}. This is the reason why the energizing time of NL0.1 and NLOR for later spray measurements are set as different.

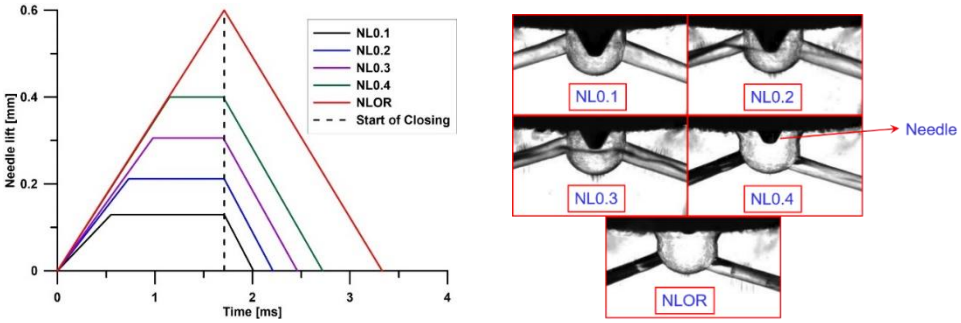

(a) Needle lift movement evolution (b) Needle lift at the start of closing

Fig. 4 effects of adjusting pad on needle lift (Pinj=70 MPa).

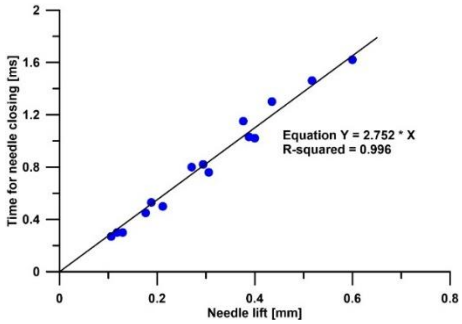

Fig. 5 Time of needle closing process with NL_{max}.

The effects of injection pressure on needle lift movement for NL0.1 and NLOR cases are presented in

Fig. 6. It can be seen that a higher injection pressure results in a higher NL_{max} and a faster opening speed because of the higher hydraulic force. However, the start of needle closing time is different, where an earlier starting time can be observed for the case with lower injection pressure. Additionally, as mentioned above, a lower NL_{max} results in a shorter closing time. Thus, lower injection pressure will lead to a shorter injection duration when keeping the same energizing time.

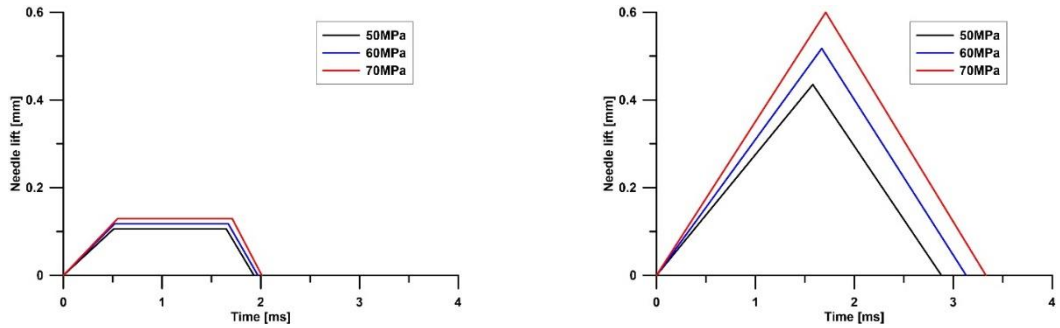

(a) NL0.1 (b) NLOR

Fig. 6 Effects of injection pressure on needle lift movement.

3.2 Effects of maximum needle lift on spray characteristics

In this section, NL0.1 and NLOR cases are compared to study the effects of NL_{max} on spray characteristics. A time sequence of reacting spray contours of these two cases under operating condition P_{inj}=100 MPa, T_a=850K, O_2 =18% are presented in Fig. 7, where the contours are derived from 50% probability maps of schlieren images. The detailed information about the processing methodology for these contours can be referenced from [26]. As shown in Fig. 7, it seems that the NL_{max} does not create significant influence on macroscopic spray geometry, no matter at the time position before autoignition (0.61 ms ASOI) or quasi-steady diffusion combustion period (2.41 ms ASOI). Only a slight radial difference can be observed between 20-30 mm, which could be caused by experimental uncertainty. The spray tip penetration at four different time positions are also quite similar.

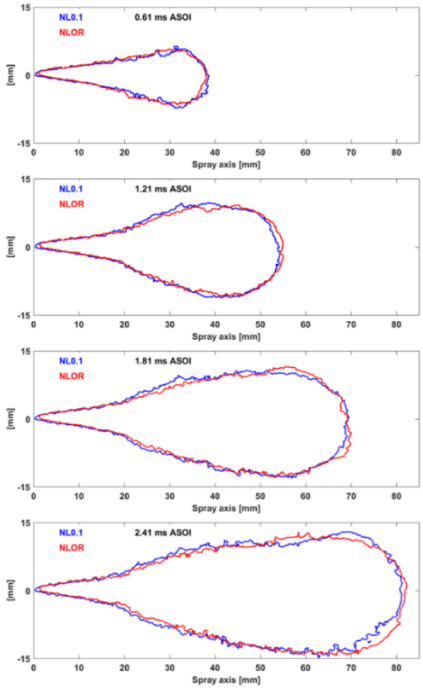

Fig. 7 Temporal evolution of reacting spray contours obtained from Schlieren techniques. The blue color and red color represent NL0.1 and NLOR cases respectively. (P_{inj} =100 MPa, T_a = 850 K, O_2 =18%)

The temporal evolution of spray tip penetration averaged over 10 repetitions as well as corresponding standard deviation are presented in Fig. 8 when the ambient temperature is at 850K. The solid lines represent NL0.1 cases and dashed lines represent NLOR cases. The penetration curves of some cases become flat at the end of time window because it reaches the limitation of optical access. It is consistent with the spray contours as shown in Fig. 7 that penetration curves are almost overlapping each other with different NL_{max} under both inert conditions and reacting conditions. It is well known that the spray penetration is mainly depended on spray momentum flux. Thus, the similarity of inert spray penetration with different NL_{max} indicates that the spray momentum flux should be similar. However, the results are inconsistent with previous work presented by R. Payri et al.[17] where a faster vapor penetration and higher mass flow rate are observed with higher needle lift. One possibility for this difference is that a multi-hole piezoelectric injector was applied in their study instead of using the vertical single-hole solenoid injector, where the effects of needle lift position on internal flow characteristics for inclined holes could be different. As presented in Fig. 4(b), the cavitation phenomenon is quite different at different needle positions.

However, the internal flow of single-hole nozzle is not able to be carried out because of experimental limitation. Thus, the relationship between internal flow and spray characteristics for vertical hole nozzles will be discussed by means of simulation in later section. Furthermore, the similarity on penetration of reacting sprays indicates the ignition delay should also be similar because of significant influence of ignition delay on spray penetration, proved by previous research [26].

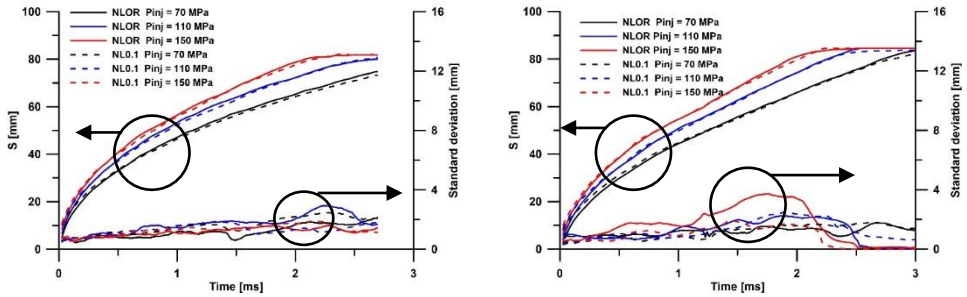

(a) Inert sprays (b) Reacting sprays

Fig. 8 Temporal spray tip penetration averaged over repetitions. The solid lines and dashed lines represent NL0.1 and NLOR cases respectively. (T_a = 850 K)

The effects of NL_{max} on ID and LOL with parametric variations are shown in Fig. 9, where these vertical bars represent standard deviations of cycle-to-cycle variations. It can be seen from Fig. 9(a)(b). that the ID decreases with higher injection pressure and higher ambient temperature, meanwhile, the LOL increases with higher injection pressure and decreases with higher ambient temperature as show in Fig. 9(c)(d), which is consistent with previous research. However, there is no remarkable difference on both ID and LOL with different NL_{max}, except the low temperature case because of unsteady flames where much higher standard deviations can be observed. It can be speculated that this similar ID and LOL are mainly contributed by similar spray dynamics as shown in Fig. 7 and Fig. 8, where the evolution of fuel-air mixture fraction should be quite similar. As a consequence, it can be concluded that under the same injection duration the maximum needle lift does not have a significant influence on spray dynamics, autoignition process and flame structure within present range of NL_{max}.

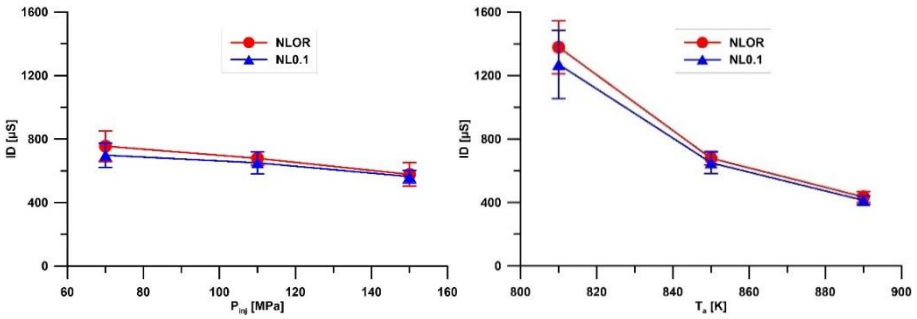

(a) ID with P_{inj} variation. (b) ID with T_a variation.

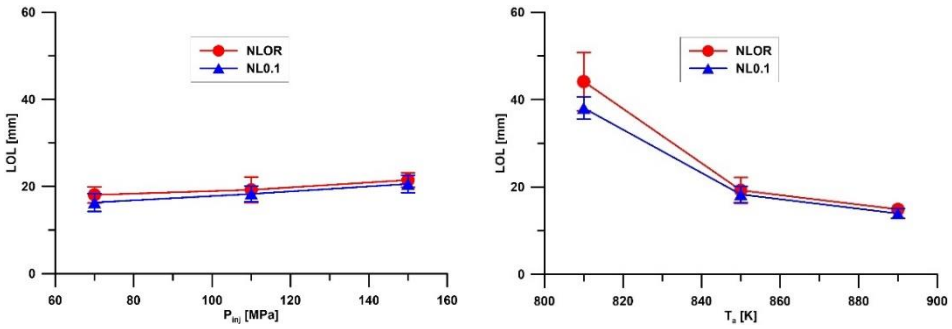

(c) LOL with P_{inj} variation. (d) LOL with T_a variation.

Fig. 9 Effects of NLmax on ID and LOL with parametric variations.

4 Discussion

In order to have a better understanding of the effects of NL_{max} on spray characteristics, a series of numerical simulations of the internal nozzle flow for this injector presented above with fixed injection pressure (P_{inj} = 110 MPa) and back pressure (P_b = 5 MPa) has been performed by means of a commercial CFD software. All simulations were performed as steady state flow, since the needle lift was kept constant as NL_{max}. The Renormalization Group (RNG) k-ε model is employed for computing the turbulent kinetic energy k and the turbulent dissipation ε. The Zwart-Gerber-Belamri (ZGB) cavitation model based on the Rayleigh-Plesset equations is applied in this study to describe the mass transfer through the interface of the vapor and the liquid. Six different NL_{max} cases have been simulated: 0.03 mm, 0.05 mm, 0.07 mm, 0.1 mm, 0.4 mm and 0.9 mm. The cell numbers of the meshes vary from $2.6x10^6$ to $2.9x10^6$ according to different NL_{max} cases.

The flow coefficients of the nozzle, namely, discharge coefficient (C_d), velocity coefficient (C_v) and area coefficient (C_a), are calculated according to the following equations:

$$C_d = \frac{\dot{m}_f}{\dot{m}_{th}} = \frac{\dot{m}_f}{A\sqrt{2 \cdot \rho_f \cdot \Delta P}} \tag{1}$$

$$C_v = \frac{V_{avg}}{V_{th}} = \frac{V_{avg}}{\sqrt{\frac{2\Delta p}{\rho_f}}} \tag{2}$$

$$C_a = \frac{C_d}{C_v} \tag{3}$$

where $\dot{m}_f$ represents calculated exit fuel mass flow and $\dot{m}_{th}$ represents theoretical exit fuel mass flux, ΔP is the pressure drop between injection pressure and back pressure, V_{avg} represents averaged flow velocity over nozzle orifice area and V_{th} represents theoretical velocity by applying Bernoulli equation between inlet and outlet of the nozzle hole and assuming the inlet velocity is negligible.

Consequently, these three flow coefficients of different NL_{max} cases are obtained as shown in Fig. 10 based on simulated averaged flow velocity and mass flux at the nozzle exit. It can be found that

discharge coefficient and velocity coefficient behave as a "knee" shape with NL_{max} and they become almost flat when NL_{max} is greater than 0.1 mm, while the area coefficient is almost kept constant within the scope of simulated NL_{max}. As a consequence, it can be used to explain the similar spray characteristics for NLOR and NL0.1 case presented above. However, the velocity coefficient decreases sharply with lower NL_{max} when NL_{max} is smaller than 0.1 mm which is mainly caused by the pressure drop across the needle seat. Apparently, there is a significant pressure drop for the smallest NL_{max} case (0.03 mm) compared to the other two cases, because the gap across the needle seat is too small and behaves as a throttle. It can be speculated that the spray characteristics would become quite different if such low NL_{max} used for spray visualization. However, the application of such low NL_{max} in real engines will be meaningless, because it will result in a quite small penetration velocity and super long injection duration when keeping the same injected fuel mass which will lead to a poor fuel-air mixing and low combustion efficiency.

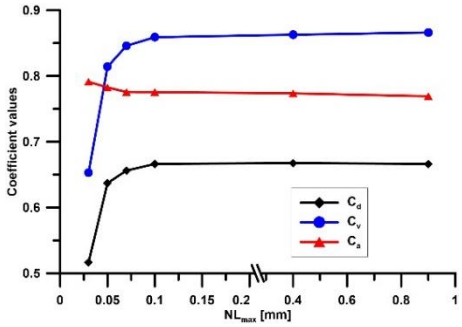

Fig. 10 Flow coefficients as a function of NL_{max}.

In present study, all the spray measurements were conducted with a vertical hole nozzle which has almost the same cavitation area with different NL_{max}, as presented in Fig. 10 where the area coefficient (C_a) is almost constant. However, the different position of needle lift could bring an important influence on the cavitation phenomenon for inclined hole nozzle or realistic commercial multi-hole nozzle, which could result in a significant difference on spray characteristics. Thus, current work presents a methodology and first step analysis on the effects of needle position on reacting spray characteristics with vertical hole nozzle, which provides a useful reference for further relevant study for inclined hole nozzles.

5 Conclusions

The needle lift profiles of a solenoid injector and its reacting spray characteristics have been able to be linked in this study. The needle movement under atmosphere pressure was measured by using an optical nozzle tip and high-speed imaging. After that, the spray visualization tests of the same injector equipped with a vertical single-hole nozzle were carried out in a constant volume combustion chamber. The most relevant observations and conclusions of this study are summarized below:

The needle lift profile of a solenoid injector has been successfully regulated by means of changing the thickness of an adjusting pad between the needle and rod within the injector. The difference on NLmax does not create a significant influence on starting time of needle closing and the closing time needed is proportional to the value of NLmax when keeping the same injection pressure.

Within presented experimental range of maximum needle lift, the difference on the needle lifting process and NL_{max} do not bring a significant difference on spray tip penetration, ignition delay and flame lift-off length for this vertical single-hole injector. It is mainly contributed by the similar spray momentum flux and evolution of fuel-air mixture fraction, which are caused by similar characteristics of internal flow within the nozzle.

The simulated results show that the discharge coefficient and velocity coefficient of internal flow behave as a "knee" shape as a function of NL_{max}. They keep almost flat when NL_{max} is greater than 0.1 mm and decrease sharply when it is smaller than 0.05 mm because of the "throttle" effect. However, the caviation area within the nozzle is almost kept constant within the scope of simulated NL_{max}.

Acknowledgements

This study was partially funded by Natural Science Foundation of Jiangsu Province (BK20190856), the Key Research and Development Program of Jiangsu Province (BE2019009-4), Jiangsu Planned Projects for Postdoctoral Research Fund (2019K035) and Senior Talent Foundation of Jiangsu University (18JDG029).

References

[1] Huang W., et al., Near-nozzle dynamics of diesel spray under varied needle lifts and its prediction using analytical model, *Fuel*, 180 (2016), pp. 292–300

[2] Desantes J.M., et al., A study on tip penetration velocity and radial expansion of reacting diesel sprays with different fuels, *Fuel*, 207 (2017), pp.323–335

[3] Shuai S., et al., Evaluation of the effects of injection timing and rate-shape on diesel low temperature combustion using advanced CFD modeling, *Fuel*,88 (2009), pp.1235–1244

[4] He Z., et al., A numerical study of the effects of injection rate shape on combustion and emission of diesel engines, *Thermal Science*, 18 (2014), pp.67-78

[5] Bruneaux G., et al., Study of the mixing and combustion processes of consecutive short double diesel injections. *SAE Int J Engines*, 2 (2009), pp.1151–1169

[6] Desantes J. M., et al., Optical study on characteristics of non-reacting and reacting diesel spray with different strategies of split injection, *International Journal of Engine Research*, 20(2019), pp.606-623

[7] Payri R., et al., The effect of nozzle geometry over the evaporative spray formation for three different fuels, *Fuel*, 188 (2017), pp.645–660

[8] Chen Z., et al., Experimental study on the effect of nozzle geometry on string cavitation in real-size optical diesel nozzles and spray characteristics, *Fuel*, 232(2018), pp.562–571

[9] Zhang L., et al., Simulations on the cavitating flow and corresponding risk of erosion in diesel injector nozzles with double array holes, *International Journal of Heat and Mass Transfer*, 124 (2018), pp.900–911

[10] He Z., et al., Experimental and numerical study of cavitation inception phenomenon in diesel injector nozzles, *International Communications in Heat and Mass Transfer* ,65 (2015), pp.117–124

[11] Liu F., et al., Microscopic study on diesel spray under cavitating conditions by injecting fuel into water, *Applied Energy*, 230 (2018), pp.1172–1181

[12] Powell C. F., et al., The Effects of Diesel Injector Needle Motion on Spray Structure, *Journal of Engineering for Gas Turbines and Power*, JANUARY 2011, Vol. 133

[13] Huang W., et al., Near-nozzle dynamics of diesel spray under varied needle lifts and its prediction using analytical model, *Fuel*, 180 (2016), pp.292–300

[14] Marti-Aldaravi P., et al., Numerical Simulation of a Direct-Acting Piezoelectric Prototype Injector Nozzle Flow for Partial Needle Lifts, *SAE Technical Paper*, 2017-24-0101, 2017

[15] Salvador F.J., et al., Study of the influence of the needle lift on the internal flow and cavitation phenomenon in diesel injector nozzles by CFD using RANS methods, *Energy Conversion and Management*, 66 (2013), pp. 246–256

[16] Payri R., et al., Study liquid length penetration results obtained with a direct acting piezo electric injector, *Applied Energy*, 106 (2013), pp.152–162

[17] Payri R., et al., Needle lift profile influence on the vapor phase penetration for a prototype diesel direct acting piezoelectric injector, *Fuel*,113 (2013), pp.257–265

[18] Xuan T., et al., A study of soot quantification in diesel flame with hydrogenated catalytic biodiesel in a constant volume combustion chamber, *Energy*, 145 (2018), pp.691-699

[19] Xuan T., et al., Effects of an injector cooling jacket on combustion characteristics of compressed-ignition sprays with a gasoline-hydrogenated catalytic biodiesel blend, *Fuel*, 276(2020)117947

[20] Benajes J., et al., Experimental characterization of diesel ignition and lift-off length using a single-hole ECN injector, *Applied Thermal Engineering*, 58 (2013), pp.554-563

[21] Payri R., et al., Diesel ignition delay and lift-off length through different methodologies using a multi-hole injector, *Applied Energy*, 162 (2016), pp.541–550

[22] Xuan T., et al., In-flame soot quantification of diesel sprays under sooting/non-sooting critical conditions in an optical engine, *Applied Thermal Engineering*, 149 (2019) 1-10

[23] Xuan T., et al., Soot temperature characterization of spray a flames by combined extinction and radiation methodology, *Combustion and Flame*, 204(2019), pp.290-303

[24] Hayashi T., et al., Effects of internal flow in a diesel nozzle on spray combustion, *International J of Engine Research* 14(2013), pp.646–654

[25] He Z.,et al., Effect of nozzle geometrical and dynamic factors on cavitating and turbulent flow in a diesel multi-hole injector nozzle, *International Journal of Thermal Sciences*,70(2013), pp.32-143

[26] Payri R., et al., A study on diesel spray tip penetration and radial expansion under reacting conditions, *Applied Thermal Engineering*, 90 (2015) 619-629

Submitted: 25.09.2019.
Revised: 29.06.2020.
Accepted: 02.09.2020.